

# Prediction of Pore Water Pressure of Iron Concentrate Using Phase Space Reconstruction Long Short-Term Memory

Senyuan LI<sup>1, a</sup>, Hang ZHOU<sup>2, a</sup>, Jianwei ZHANG<sup>3, a</sup>, Jian LIU<sup>4, b</sup>

<sup>a</sup>*School of Naval Architecture and Maritime Zhejiang Ocean University Zhoushan 316022, China*

<sup>b</sup>*China Classification Society Guangzhou Branch China Classification Society Guangzhou 510235, China*

**Abstract.** Ship shaking can cause cargo PWP (pore water pressure) increasing, the prediction of PWP is helpful for navigation safety. This paper presents a machine learning method for PWP time series prediction learning. Source data of iron concentrate are collected from scaled model test, they are used to train a time series prediction model and test the accuracy and effective of our method. The proposed method is based on PSR (phase space reconstruction) and LSTM (Long Short-Term Memory) Network. A input matrix is constructed by phase space reconstruction technology and the prediction model can be learned by a specific Long Short-Term Memory Network. The single-step pore water pressure prediction model is achieved, when MSE loss function value is minimum, the R value 0.98 is maximum is better than the baseline R value 0.93. This result suggests that this PSR-LSTM is more effective than LSTM, it can be a complement for physical test and numerical simulation.

**Keywords.** navigation safety; machine learning; phase space reconstruction; LSTM; time series prediction

## 1. Introduction

The granular bulk cargo is mainly transported by ship. Because of shaking of ship motion, the risk of liquefaction during shipping is increasing. From 2010 to 2020, cargo liquefaction caused many accidents, the number of it is more than 32 in China [1].

Many researches give evidence that liquefaction of cargo is accompanied by an increase in PWP [2]. So, the PWP in granular bulk cargo is often used to predict the cargo liquefaction [3]. Therefore, an accurate prediction of shaking-induced PWP is significant for navigation safety. Numerous numerical studies for ship–cargo interactions have been reported. Based on UBC3D-PLM constitutive model, [4] assess cargo liquefaction

---

<sup>1</sup> Senyuan LI, School of Naval Architecture and Maritime Zhejiang Ocean University Zhoushan 316022, China; email: lisenyuan@zjou.edu.cn

<sup>2</sup> Hang ZHOU, School of Naval Architecture and Maritime Zhejiang Ocean University Zhoushan 316022, China; email: 1223490491@qq.com

<sup>3</sup> Corresponding author: Jianwei ZHANG, School of Naval Architecture and Maritime Zhejiang Ocean University Zhoushan 316022, China; email: zhangjianwei@zjou.edu.cn

<sup>4</sup> Jian LIU, China Classification Society Guangzhou Branch China Classification Society Guangzhou 510235, China; email: jianliu@ccs.org.cn

potential. Reference [5] discussed the application of another constitutive model named UBCSAND. Experimental studies [6] mainly include scaled cargo hold model tests and [7] one-dimensional material column tests. However, these physical and numerical prediction models are not adoptable to quickly and conveniently make prediction.

Increasing data volumes are driving new technologies, it helps us directly extract prediction models from raw data [8]. Machine learning is increasingly used in engineering [9]. Reference [10] used an RNN-based model to predict the hydrodynamic load generated by liquid storage tanks, and compared with the test results. Reference [11] predicted the dynamic mooring line response in real time through the LSTM neural network model.

This article will try to make a prediction model for PWP based on the actual experimental measurements. The proposed machine learning method including PSR technology and LSTM. The next content includes three parts: Section 2 introduces the steps of the PSR-LSTM method. Next, Section 3 show, compare and discuss the prediction result of LSTM and PSR-LSTM. Finally, Section 4 summarizes the conclusions.

## 2. Methodology

This section shows the steps for constructing prediction model of PWP. They are PWP collection, time series reconstruction, and Long Short-Term Memory Network.

### 2.1. Step 1: PWP collection

Vibrating Wire Piezometer were used to measure the PWP change in scaled model. The experimental facility and scaled model are shown in Fig. 1. The iron samples were collected from the Laotangshan, Zhejiang province. Acceleration, frequency of shaking table and the percentage of water content of iron concentrate are considered.  $x(t)$  is the PWP value at time  $t$ . The purpose for collecting different time  $x(t)$  is to make a prediction model, the prediction model can be written (1) as following:  $f$  is the objective prediction model for  $(x_1, \dots, x_n)$ .  $y(t)$  is the time series of PWP.

$$y(t)=f(x_1, \dots, x_{n-1}, x_n) \quad (1)$$



**Figure. 1** Six degrees of freedom shaking table and cargo hold model.

2.2. Step 2: Time Series Reconstruction

According to Takens embedding theorem, PWP includes some hidden information, such as strain-stress response of cargo. To better model the collected time series, we consider the application of phase space reconstruction expressed in (2), structuring data dimension by stacking the state variable vector at fixed time instances:

$$X(t) = [x_t, x_{(t+\tau)}, \dots, x_{(t+(d-1)\tau)}] \tag{2}$$

$X(t)$  is the collection result in step 1, where  $\tau$  is the delay step controlling the time interval,  $d$  represents embedding dimension controlling number of columns of  $X(t)$ . The selection of  $\tau$  and  $d$  is important, the reconstruction accuracy is related to these parameters. In this paper, both the mutual information (MI) and the false nearest neighbors (FNNs) method will be used to determine these two parameters.

2.3. Step 3: LSTM Network

The conditions of the Takens embedding theorem are satisfied, the result (3) of time series reconstruction consisting of reconstructed state vector as following, where each row in this matrix called state vector, each vector is  $d$  dimension, comparing with single 1-dimension pore water pressure value, the state vector represents more information.

$$\begin{bmatrix} X_1 & X_{(1+\tau)} & \dots & X_{(1+(d-1)\tau)} \\ X_{(1+\tau)} & X_{(1+2\tau)} & \dots & X_{((1+\tau)+(d-1)\tau)} \\ \vdots & \vdots & \ddots & \vdots \\ X_{(1+q\tau)} & X_{(1+(q+1)\tau)} & \dots & X_{((1+q\tau)+(d-1)\tau)} \end{bmatrix} \tag{3}$$

The prediction model will be constructed, considering the time feature of pore water pressure, we will develop a LSTM Memory Network to learn a prediction model. Because of the extended memory block with a storage unit, LSTM has strong time awareness ability in time series processing, it can learn how long to retain state information. A stacked LSTM structure in Fig. 2 is defined as a deep learning model composed of multiple LSTM layers, every input time steps correspond to one output value. Hidden layers of stacking LSTM give the model more depth, it can better fit the change law of sequence data.

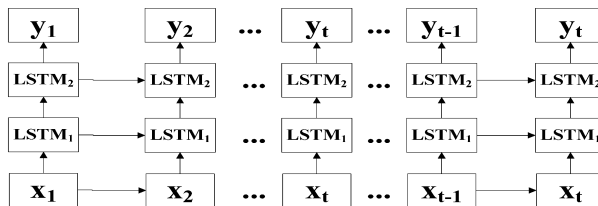


Figure. 2 Structure of stacking Long Short-Term Memory Network.

3. Results and Discussion

The calculating processing is in Fig. 3.

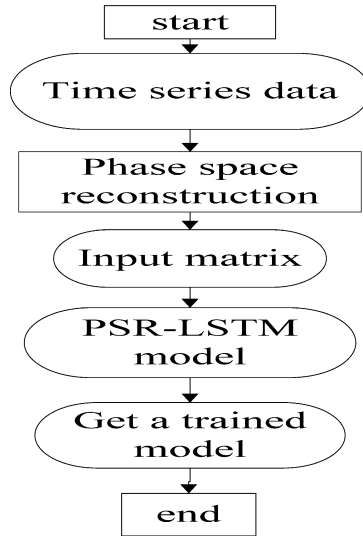


Figure. 3 The training process of proposed method.

### 3.1. Data Collection Result

Ship rolling is simulated by horizontal motion of shaking table. The selected motion frequency is 1Hz and acceleration is 0.5g. Cargo hold model is partially filled with iron concentrate ore sample with 10% water content, the load depth is 0.25 m. A pore-water pressure sensors (PDCR81) located in the middle of the model at a distance of 0.1cm from the iron surface to track the evolution of the pore-water pressure increasing. A PWP is recorded in Fig. 4. On the first stage, the signal is transient back and forth fluctuations, pore water pressure is not accumulation, soil is mainly elastic deformation. On the second stage, the signal is not only transient back and forth fluctuations, but also average monotonic cumulative increasing, soil is elastoplastic deformation. On the third stage, the signal is undulating change in the time domain. Without external load, the signal falls to initial value, excess water pore pressure is dissipation.

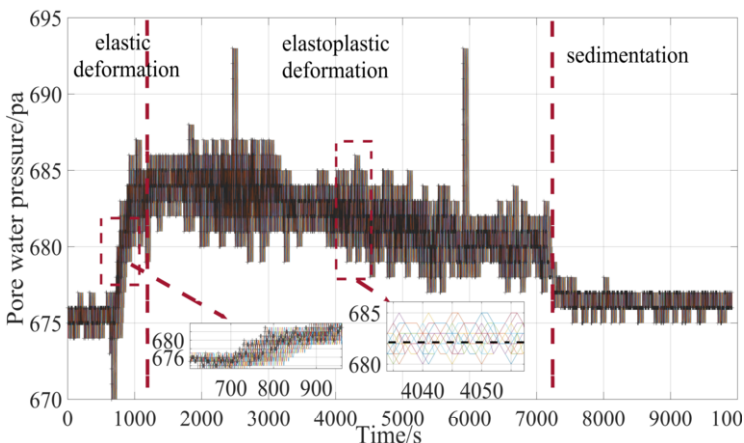


Figure. 4 The pore water pressure sequence collection result.

### 3.2. Time Series Reconstruction Result

The delay step  $\tau$  is defined by the AMI value. First, probabilities  $p(x_t)$ ,  $p(x_{t+\tau})$  and  $p(x_t, x_{t+\tau})$  in the computation of AMI for different  $\tau = \Delta t, 2\Delta t, \dots, 20\Delta t$  have been estimated. Fig.5 shows the computed AMI values. The first minimum AMI value occurs at  $\tau = 5\Delta t$ . Therefore, the delay step is 5. Fig. 6 shows the selection result for  $d$ . when  $d$  is 17, percentage drop exceeds 90%, indicating the dimension can smoothly unfold the PWP.

After defining the above two parameters, we can assemble the input matrix as (3), as input for machine learning. The reconstructed result is plotted in three-dimensional in Fig. 7.

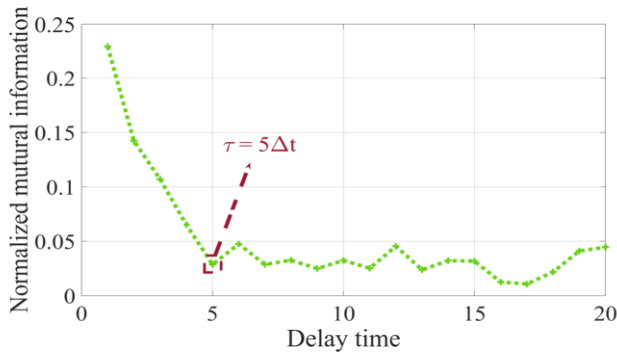


Figure. 5 Selection result of delay step  $\tau$ .

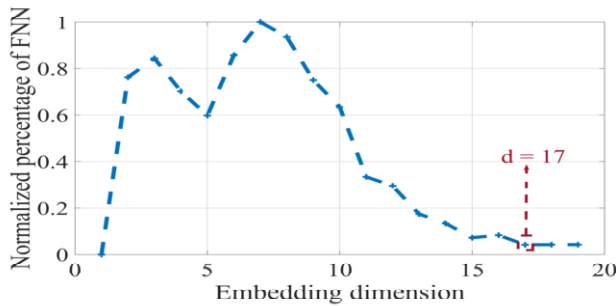


Figure. 6 Selection result of embedding dimension  $d$ .

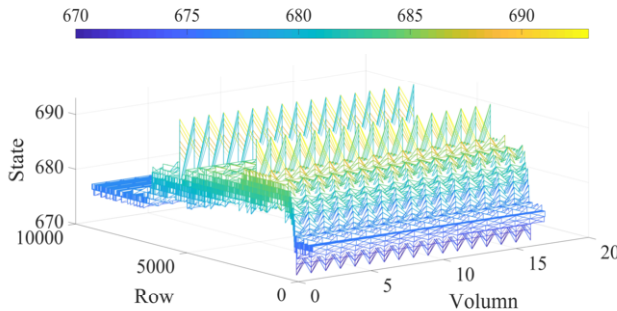


Figure 7 Reconstructed result in three-dimensional space.

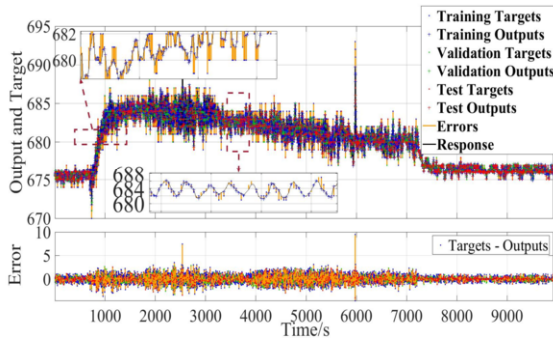


Figure. 8 Learned result based on PSR-LSTM.

### 3.3. PSR-LSTM Learning Results

LSTM and PSR-LSTM are respectively used to compared with the prediction performance. 70% data is training data, this part is used to calculated the parameters of a prediction model and get a convergent model, 15% data is validated data, this part of the data is used to calculate the generalization of the network. 15% data is test data, these are independent of the training data and are used to evaluate the performance of the trained predictive model. Shown in Fig. 8, learned result from the PSR-LSTM is closer to real data change, back and forth fluctuations have been well predicted, in comparison with Fig. 9, as a result, the feature of soil deformation can be learned by the PSR-LSTM prediction model. The input matrix can provide the LSTM with more information that is hidden in initial time sequence. In conclusion, with the same structure network, the PSR-LSTM prediction model is more accurate than the LSTM prediction model.

The training performance in Fig. 10, Fig. 11. MSE (mean squared error) is the average squared difference between prediction result and target result. The MSE is more lower, the performance is more better. The PSR-LSTM has better test performance, MSE is 0.3683, at epoch 6. LSTM MSE is 1.3111, at epoch 68, clearly the PSR-LSTM has faster convergence, so it is more effective for predicting pore water pressure.

According to the correlation between prediction result and target result. If the R is 1, it means there is a close relationship between them, if R is 0, it means a random relationship. The result is in Fig. 12, Fig. 13, R is 0.93 for LSTM and R is 0.98 for PSR-LSTM. There is about 5% increase of R value. In conclusion, the output correctness of PSR-LSTM is also better LSTM.

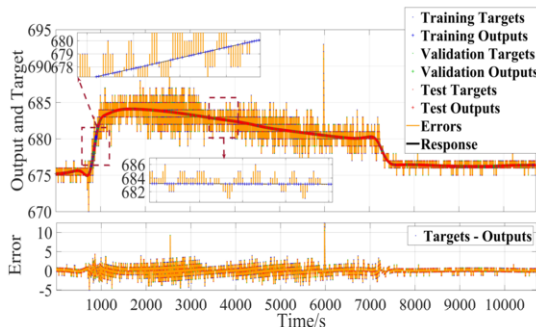


Figure. 9 Learned result based on LSTM.

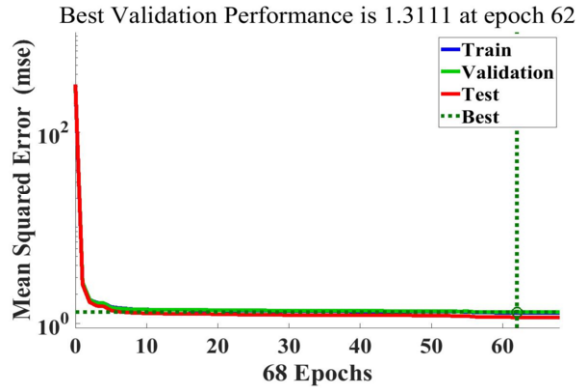


Figure. 10 MSE for LSTM.

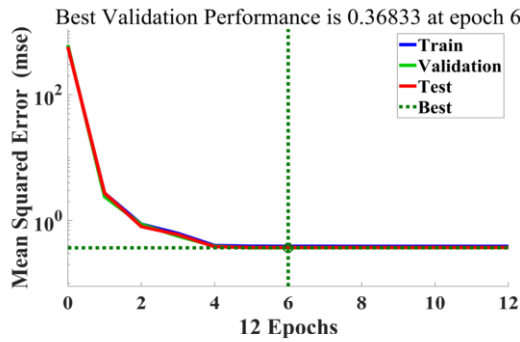


Figure. 11 MSE for PSR-LSTM.

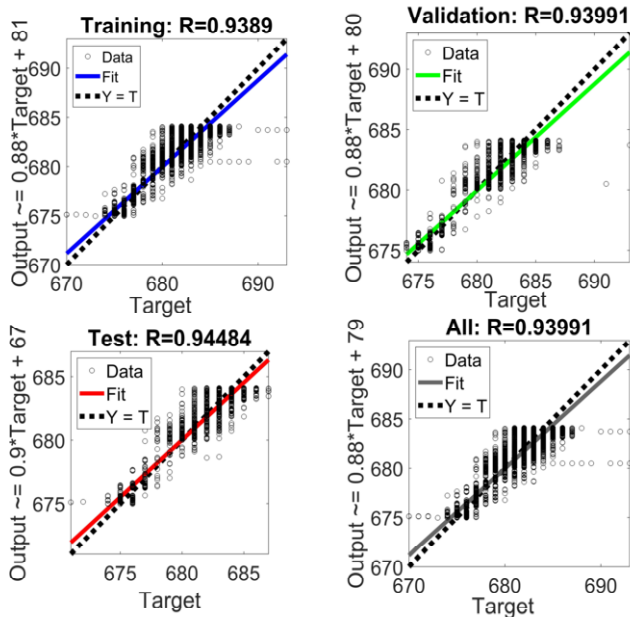


Figure. 12 R Values for LSTM.

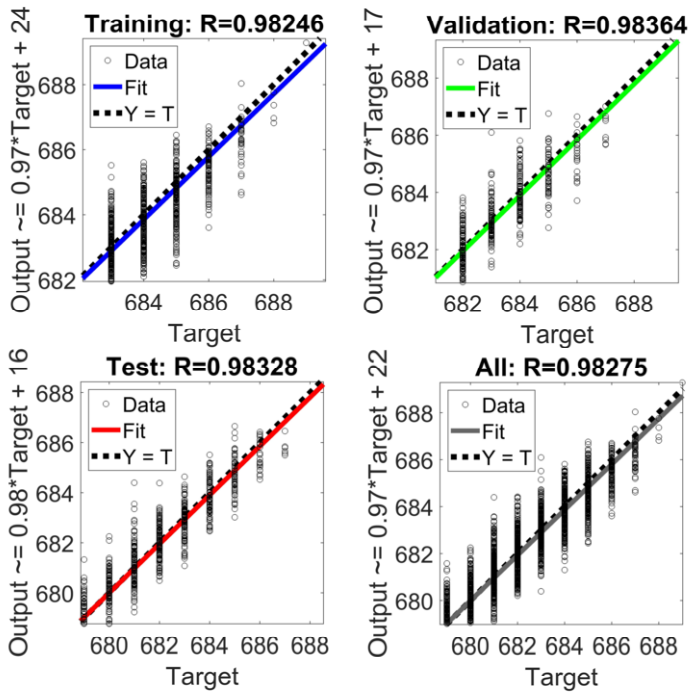


Figure. 13 R Values for PSR-LSTM.

#### 4. Conclusion

This paper proposes a machine learning method predicting the pore water pressure of liquefied iron concentrate cargo. In comparison to traditional time sequence prediction methods LSTM, the proposed machine learning method provides reconstructed state matrix to gain relevant information of dynamic system. After, LSTM is utilized to learn a prediction model. Comparing with directly using LSTM, the PSR-LSTM is more effective and accuracy, it is an excellent candidate for applied in actual transportation and helpful to guide engineers to make more reasonable strategies for navigation safety.

#### Acknowledgment

This research was financially supported by the National Natural Science Foundation of China (Grant No. 51809237) and the Fundamental Research Funds for the Provincial Universities (Grant No. 2021J017).

#### References

- [1] Wu, W. et al. (2022) Quantitative analysis of liquefaction risk of liquefiable solid bulk cargoes during sea transport. *Ocean Engineering*, 258:111751. <https://doi.org/10.1016/j.oceaneng.2022.111751>
- [2] Cui, J., S. Dong, Z. Wang, J. Cheng, and J. Ren. (2022) Experimental study on motion response of a

- submersible spherical model under the action of internal solitary wave propagating over a ridge topography. *Ocean Engineering*, 258:111700. <https://doi.org/10.1016/j.oceaneng.2022.111700>
- [3] Cheng, H., Y. Cheng, Y. Zheng, J. Zhang, and X. Lyu. (2023) Prediction of irregular wave (current)-induced pore water pressure around monopile using machine learning methods. *Coastal Engineering*, 182:104291. <https://doi.org/10.1016/j.coastaleng.2023.104291>
- [4] Chakraborty, A. and V. A. Sawant. (2023) Fragility assessment of highway embankment resting on liquefaction-susceptible soil. *Computers and Geotechnics*, 161: 105568. <https://doi.org/10.1016/j.compgeo.2023.105568>
- [5] Voyagaki, E., T. Kishida, R. F. Aldulaimi, and G. Mylonakis. (2023) Integration and calibration of UBCSAND model for drained monotonic and cyclic triaxial compression of aggregates. *Soil Dynamics and Earthquake Engineering*, 171:107978. <https://doi.org/10.1016/j.soildyn.2023.107978>
- [6] Xu, X., Y. Ren, Q. Meng, H. Wu, and G. Xu. (2022) Force on structures caused by oscillation of liquefied silty soil. *Ocean Engineering*, 258:111634. <https://doi.org/10.1016/j.oceaneng.2022.111634>
- [7] Zhang, Y. et al. (2022) An optimal statistical regression model for predicting wave-induced equilibrium scour depth in sandy and silty seabeds beneath pipelines. *Ocean Engineering*, 258:111709. <https://doi.org/10.1016/j.oceaneng.2022.111709>
- [8] Ashouri, M., N. Kheyrikoochaksarayee, C. Chhokar, A. Shabani, and M. Bahrami. (2023) A big data-handling machine learning model for membrane-based absorber reactors in sorption heat transformers. *Energy Conversion and Management*, 292: 117376. <https://doi.org/10.1016/j.enconman.2023.117376>
- [9] Zheng, L., C. Wang, X. Chen, Y. Song, Z. Meng, and R. Zhang. (2023) Evolutionary machine learning builds smart education big data platform: Data driven higher education. *Applied Soft Computing*, 136:110114. <https://doi.org/10.1016/j.asoc.2023.110114>
- [10] Xie, Y., H. Tang, and Y. M. Low. (2023) Deep gated recurrent unit networks for time-domain long-term fatigue analysis of mooring lines considering wave directionality. *Ocean Engineering*, 284: 115244. <https://doi.org/10.1016/j.oceaneng.2023.115244>
- [11] Shi, W., L. Hu, Z. Lin, L. Zhang, J. Wu, and W. Chai. (2023) Short-term motion prediction of floating offshore wind turbine based on multi-input LSTM neural network. *Ocean Engineering*, 280: 114558. <https://doi.org/10.1016/j.oceaneng.2023.114558>